

1 **Title page**

2 **Working title:** páramo assemblages Andes

3 **Full title:**

4 **The fate of páramo plant assemblages in the sky islands of the northern Andes**

5 **Authors:**

6 Gwendolyn Peyre¹, Jonathan Lenoir², Dirk N. Karger³, Monica Gomez¹, Alexander
7 Gonzalez¹, Antoine Guisan⁴

8 ¹ Department of Civil and Environmental Engineering, University of the Andes, Bogotá,
9 Colombia

10 ² Université de Picardie Jules Verne - CNRS, Amiens, France

11 ³ Swiss Federal Research Institute WSL, Birmensdorf, Switzerland

12 ⁴ Université de Lausanne, Lausanne, Switzerland

13 **Correspondence:**

14 Gwendolyn Peyre, Department of Civil and Environmental Engineering, University of the
15 Andes, Bogotá, Colombia

16 Email address: gf.peyre@uniandes.edu.co

17 **Funding information**

18 GP was financed through the Fondo de Apoyo para Profesores Asistentes – FAPA of the
19 University of the Andes [PR.3.2016.3708].

20

21 **Abstract**

22 *Aims:* Assessing climate change impacts on biodiversity is a main scientific challenge,
23 especially in the tropics, therefore, we predicted the future of plant species and communities
24 on the unique páramo sky islands. We implemented the *Spatially Explicit Species*
25 *Assemblage Modelling* framework, by i) calculating species' maximum dispersal distance,
26 ii) modelling species distributions at present up to 2100, iii) assembling models into
27 communities. Finally, we assessed the vulnerability of sky islands based on richness and
28 composition changes.

29 *Location:* Ecuadorian super-páramo (>4200 m)

30 *Methods:* Using species trait data, the maximum dispersal distance of 435 species was
31 calculated. Species distribution models (SDM) were fitted to obtain current and future
32 distribution predictions based on dispersal and bioclimatic factors. The final assemblages
33 for present and 2100 were achieved by stacking all probabilistic SDMs and applying the
34 probability ranking rule. The vulnerability of each sky island was evaluated by quantifying
35 richness and composition changes.

36 *Results:* Maximum dispersal distances ranged between 0.008-6027 m/year, and across all
37 scenarios, 70% of models showed a net loss in species distribution while 9% of all species
38 were predicted to undergo extinction by 2100. Local richness was estimated to decrease by
39 56.63% on average, and composition changes in each sky island suggested a mean loss of
40 64.74% of their original species pool against a 12.97% gain. Finally, 5% of the sky island
41 floras reconverted from high-elevation to low-elevation species. These numbers were
42 usually more important for high-elevation species and the mountains Pichincha, Ilinizas and
43 Antisana.

44 *Conclusions:* Our study is methodologically pioneer and provides novel insight on the future
45 of páramo biodiversity. Significant losses in species distribution and changes in community
46 richness and composition suggest drastic impacts and call for further study considering
47 additional factors, such as land-use. Finally, we recommend focusing monitoring and
48 conservation strategies on the northern sky islands in priority.

49 **Key words:** Andes, community assemblages, climate change, maximum dispersal
50 distance, páramo, plant species, Species Distribution Models, Spatially Explicit Species
51 Assemblage Modelling, sky islands.

52

53 **Introduction**

54 The climatically-driven redistribution of life on Earth is one of the most challenging
55 environmental threat humanity faces today (Pecl et al. 2017; Diaz et al. 2019). It is widely
56 accepted that the current climate change is human-induced (Team et al. 2014) and that its
57 main impacts on biodiversity include: shifts in phenology (Visser, & Both, 2005); changes
58 in population densities (Graae et al. 2018), local extinctions (Panetta, Stanton, & Harte,
59 2018), species range shifts (Lenoir, & Svenning 2015), and accelerated changes in species
60 richness and assemblages (Bertrand et al. 2011; Steinbauer et al. 2018). Because biodiversity
61 redistribution implies important changes in ecosystem functioning, human well-being and
62 climate change itself (Pecl et al. 2017), there is an urgent need to increase our knowledge on
63 the complex interplay between climate change and biodiversity and implement integrative
64 scientifically-supported strategies to adapt and mitigate climate change (Diaz et al. 2019).

65 The high-elevation ecosystems in the northern Andes belong to the páramo
66 biogeographical province, a tropical biodiversity hotspot critically threatened by climate
67 change (Tovar, Arnillas, Cuesta, & Buytaert, 2013; Cuesta et al. 2019). The páramo is the
68 youngest biodiversity hotspot and the richest tropical alpine province on Earth, totaling 15
69 different phytogeographical units and around 5000 plant species, of which 60-80% are
70 endemic (Sklenář, Hedberg, & Cleef, 2014; Peyre, Balslev, & Font, 2018). It can be
71 altitudinally divided at present into three main elevation belts: i) the sub-páramo (~ 3000-
72 3500 m) or lower tree or shrub-dominated ecotone with Andean forests; ii) the mid-páramo
73 (~ 3500-4200 m), or páramo proper, including vast grasslands and giant rosette
74 communities; and iii) the super-páramo (> 4200 m), with gradually scattering vegetation
75 (Cuatrecasas, 1958). Contrarily to the sub-páramo and mid-páramo, which show certain
76 spatial connectivity and are strongly shaped by human activities, the super-páramo is,
77 hitherto, geographically isolated and above the current agriculture frontier (~ 4200m). The
78 super-páramo hence represents the iconic sky islands of the northern Andes and hosts a very
79 rare and endemic biodiversity with little species migration capacity on mountain tops.

80 Recent estimations predicted a temperature rise of 3°C (\pm 1.5) across the páramo by
81 the end of the century, accompanied by a general increase up to + 300 mm in vertical
82 precipitation (rain), however highly variable depending on geography and topography
83 (Urrutia, & Vuille, 2009; Anderson et al. 2011; Buytaert, Cuesta-Camacho, & Tobón, 2011).
84 Although there is a general consensus on the need to increase our knowledge on the climate
85 change impacts on the páramo biota and ecosystems, studies remain very scarce to date
86 (Tovar et al. 2013; Feeley, Stroud, & Perez, 2017; Anthelme, & Lavergne, 2018; Anthelme,

87 & Peyre, 2019). For instance, Anderson et al. (2011) predicted a general upslope migration
88 of 600 m for species to track the isotherms throughout the Tropical Andes by 2100. Other
89 studies have also predicted up to a 50-60% increase in threats and local extinction risks by
90 the second half of the century in the region (Ramírez-Villegas et al. 2014). At the ecosystem
91 level, changes in structure and functions are suggested for the Tropical Andes (e.g. Tovar et
92 al. 2013; Cuesta et al. 2019) but lack proper quantification for the páramo alone, and the
93 consequent impacts on species assemblages and ecosystem services remain unclear
94 (Buytaert et al. 2011). In order to fill the important knowledge gap on species redistribution
95 under anthropogenic climate change and the subsequent structural re-organisation of plant
96 assemblages in the páramo, new endeavors such as the Institute von Humboldt's Biomodels
97 (<http://biomodelos.humboldt.org.co>) or the Pontificia Católica Universidad del Ecuador's
98 Bioweb (<https://bioweb.bio>), as well as individual research initiatives (e.g. Ramírez-Villegas
99 et al. 2014), looking to model the potential distribution of páramo species under climate
100 change using species distribution models (SDMs) fitted on bioclimatic data are increasing.

101 Dispersal is key in enabling species to track climate change, essentially through the
102 mechanisms of seed production, migration over certain dispersal distance and along suitable
103 habitat routes, germination and establishment (Kammer, Schöb, & Choler, 2007; Vittoz, &
104 Engler, 2007; Lenoir, & Svenning, 2015). This factor prevails in alpine areas where plants
105 face many challenges to disperse upslope or across mountains, this due to i) often reduced-
106 dispersal capacity (Vittoz, Dussex, Wassef, & Guisan, 2009; Morgan, & Venn, 2017), ii) the
107 presence of biogeographic barriers such as forests and valleys, and iii) steep gradients
108 favouring certain dispersal paths (Dirnböck & Dullinger 2004; Engler, Hordijk, & Guisan,
109 2012). Accounting for dispersal when studying changes in species distribution in tropical
110 mountains over time is crucial, because in comparison to higher latitudes, plants' dispersal
111 capacities tend to be greater and more diverse (Chen, Tamme, Thomson, & Moles, 2019)
112 while spatial climatic variations are less pronounced. At the community level, the resulting
113 persistence vs. migration mismatch between local species, competitive regional pool and
114 newcomers, such as invasive species, translates in important restructuring and composition
115 changes (Singer et al. 2016; Alexander et al. 2018). Despite the general agreement on the
116 need to include dispersal capacity in SDMs to improve current and future species distribution
117 predictions (Araújo, & Guisan, 2006; Thuiller et al. 2008; Dullinger et al. 2012; Hattab et
118 al. 2017), this factor remains overlooked today. Moreover, when accounted for, it usually
119 takes the form of an “all or nothing” parameter, i.e. no dispersal or full dispersal (Guisan, &

120 Thuiller, 2005; Araújo et al. 2006; Holloway et al. 2016), albeit partial dispersal scenarios
121 based on mean and/or maximum dispersal distance often are more reliable (Dullinger et al.,
122 2012; Engler et al. 2012; Bateman, Murphy, Reside, Mokany, & VanDerWal, 2013).
123 Nevertheless, partial dispersal approaches are increasing thanks to new techniques allowing
124 to calculate significant approximations of dispersal distances based on a suite of plant trait
125 data (Vittoz & Engler, 2007; Thomson, Moles, Auld, & Kingsford, 2011; Tamme et al. 2014;
126 Bullock et al. 2017). Among the most dependable traits used to date is plant height, assuming
127 that a tall plant disperses further than a short one (Muller-Landau, Wright, Calderón, Condit,
128 & Hubbell, 2008; Thomson et al. 2011). Seed mass has also been evaluated as a significant
129 trait, generally suggesting that light seeds disperse further than heavy ones (Parolo, & Rossi,
130 2008), even though this pattern can be significantly influenced by the correlation between
131 plant height and seed mass (Moles, Falster, Leishman, & Westoby, 2004; Thomson et al.
132 2011). Finally, dispersal syndrome is usually considered important as, for instance flight-
133 enhancing structures may increase anemochorous dispersal, and fruit characteristics can
134 influence zoochorous dispersal (Vittoz, & Engler, 2007; Tamme et al. 2014; Thomson,
135 Letten, Tamme, Edwards, & Moles, 2017).

136 Yet, to go beyond individual species predictions from SDMs, recent scientific
137 advances in ecology propose to model entire biotic communities, relying on species
138 distributions and adding a frame of abiotic and biotic factors such as historical-dispersal
139 constraints, ecosystem richness capacity and biotic interactions among species (Guisan, &
140 Rahbek, 2011; Wisz et al. 2013; Mod, le Roux, Guisan, & Luoto, 2015). In this context, the
141 *Spatially Explicit Species Assemblage Modelling* framework (SESAM; Guisan, & Rahbek,
142 2011) has been extensively used to predict species assemblages on a wide range of
143 taxonomic groups, from insects to plants, and for several habitats, from forests to grasslands
144 (e.g. D'Amen, Pradervand, & Guisan, 2015a; D'Amen et al. 2015b; Mod et al. 2015;
145 D'Amen, Rahbek, Zimmermann, & Guisan, 2017; Mateo, Mokany, & Guisan, 2017). A
146 wealth of research efforts has focused on improving the different aspects of SESAM, either
147 regarding the macroecological constraints that represent the carrying capacity of
148 communities (D'Amen et al. 2015a; Mateo et al. 2017), or the assembly rules that prioritize
149 certain species co-occurrences (Wisz et al. 2013; D'Amen et al. 2015b). However, the
150 historical-dispersal constraints remain overlooked to date and the need persists to improve
151 techniques and launch more integrative models to refine community modelling at present
152 and under climate change scenarios (D'Amen et al. 2017; Guisan et al. 2019).

153 The present study aims at implementing the SESAM framework, accounting for
154 dispersal constraints for the first time, to predict changes in plant distributions and
155 assemblages of the páramo sky islands during the 21st century. First, maximum dispersal
156 distances were calculated and compared for mid-páramo and super-páramo species. It was
157 expected that tall species such as shrubs that present either light seeds and dispersal-
158 enhancing structures, e.g. wings, or heavy seeds with fruits dispersed by efficient zoochory,
159 e.g. by birds, would be the best dispersing species. Second, the current and future
160 distributions of each species up to the year 2100 were modelled based on bioclimatic
161 variables while accounting for dispersal constraints to explore migration and extinction rates
162 in the páramo. It was assumed that mid-páramo species would migrate further and faster
163 than super-páramo species, which would in turn present greater extinction risks. Third,
164 current and future plant communities were assembled on the sky islands by stacking all
165 previous probabilistic models and applying richness constraints and assembly rules. The
166 vulnerability of the network of sky islands was assessed based on the magnitude of changes
167 in species richness and species composition in terms of species numbers and ratio of mid-
168 páramo and super-páramo species, expecting that locally diverse areas today (Peyre, Balslev,
169 Font, & Tello, 2019) would suffer faster and more drastic changes.

170 **Methods**

171 Study area

172 Ecuador was set as study case as a model representant of páramo countries due to its
173 abundance of páramos and equatorial geolocation. The most representative mountains
174 carrying the super-páramo belt, or sky islands, in Ecuador are from North to South:
175 Cayambe, Antisana, Pichincha, Ilinizas, Cotopaxi, Chimborazo, Tungurahua, Sangay and
176 Cajas (Fig. 1A). The super-páramo is usually found between 4200-4800 m a.s.l, although its
177 lower and upper limits as well as main vegetation strongly depend on local topography and
178 topoclimate. For example, low shrublands and cushion communities can be found at lower
179 elevations under a dense upper cloud elevation zone, while meadows, deserts with shrubs
180 and periglacial deserts are most likely to occur in the higher areas shaped by volcanic activity
181 and/or glacier melting (Fig. 1B; Sklenář, & Ramsay, 2001). To conduct the following
182 modelling analyses, the 4200 m isohypse and mountain tops were assumed as the lower and
183 upper limits of the actual super-páramo belt respectively. Similarly, the 3000 m isohypse
184 was set to delimit the broader páramo province (mid-páramo plus super-páramo), in order to

185 consider upward migration of plant species from the mid-páramo to the super-páramo as
186 climate will warm under future scenarios.

187 Vegetation data

188 All vegetation plots corresponding to the Ecuadorian páramo were downloaded from
189 VegParamo, an open access database for floristic and vegetation páramo data, compiling
190 information from 40 data sources (www.vegparamo.com; Peyre et al. 2015). Because
191 VegParamo comprises the original authors' classification of the plots into sub-páramo, mid-
192 páramo, super-páramo and azonal vegetation, i.e. *Polylepis forests*, bogs and marshes and
193 rupicolous vegetation, only the plots belonging to the zonal mid-páramo and super-páramo
194 elevational belts were retained. Plots located outside the study area, e.g. on Amazonian
195 mountains, were also removed, as well as plots with a coarse georeferencing precision
196 superior to 1km in the UTM system. The final plots, all sampled according to the
197 phytosociological method (Braun-Blanquet, 1964), were rescaled into presence/absence
198 data.

199 The floristic contents of the plots were checked, and the following groups were
200 eliminated from the dataset: pteridophytes, bryophytes, lichens and vascular plants
201 determined at the genus level or higher. When a taxon was determined at the infra-specific
202 level, such as varieties and subspecies, it was aggregated at the species level. Taxonomic
203 synonymy was checked using the Plant List (www.plantlist.com) and Tropicos
204 (www.tropicos.org). Because the consequent vegetation dataset showed an important
205 imbalance of species presences versus absences, additional occurrence data was
206 complemented for these species from biological and herbarium databases consulted online,
207 including Tropicos, Aarhus University Herbarium (www.aubot.dk) and GBIF
208 (www.gbif.org). The additional occurrence data was revised to remove outlier points and
209 check duplicates between occurrence data and vegetation plots (based on UTM coordinates).
210 Decimal spatial coordinates were then obtained for all plots, using the centroid of the
211 corresponding UTM cell, as well as for the new added occurrence data, relying on the
212 original georeferencing. Species that still presented less than 6 occurrences were removed
213 and the complete dataset includes 642 vegetation plots from VegParamo (157 UTM) and
214 2095 additional occurrences for 435 vascular plant species (Fig. S1; Table S1, S2; Peyre,
215 2020). Finally, species were classified into super-páramo and mid-páramo species, when at
216 least 50% of their occurrence data occurred above and below the 4200 m isohypse,
217 respectively, resulting in 84 super-páramo species and 351 mid-páramo species.

218 Bioclimatic data

219 19 bioclimatic variables were downloaded from the CHELSA V1.2 database ([www.chelsa-](http://www.chelsa-climate.org)
220 [climate-org](http://www.chelsa-climate.org); Karger et al. 2017) and adjusted to the study area. All variables were obtained
221 for the period 1979-2013 and averaged across this time interval, considered as the current
222 conditions (year 2000), which fitted the occurrence and vegetation data (1976-2014).
223 Multicollinearity between variables was evaluated using a variance inflation factor
224 correlation analysis (*vif* function, *usdm* R package; Naimi et al. 2014), and all variables
225 below a threshold value of 0.7 for the Pearson correlation coefficient were retained
226 (Dormann et al. 2012), resulting in the following selection: mean diurnal temperature range
227 (bio2); temperature seasonality (bio4); mean temperature of the wettest quarter (bio8);
228 precipitation seasonality (bio15); and precipitation of the coldest quarter (bio19). This set of
229 predictor was not fitted per species (D'Amen et al. 2015a; Araújo et al. 2019) but was
230 considered appropriate for the study area as a whole because of its certain focus on
231 precipitation-related factors and seasonality, which usually prevail as drivers of plant
232 diversity variation in tropical mountain areas (Peyre et al. 2019). To represent future
233 scenarios and in order to encompass sufficient variance while reducing uncertainty in
234 predictions (Thuiller, Guéguen, Renaud, Karger, & Zimmermann, 2019), a total of 8 climate
235 change scenarios were selected, based on two representative concentration pathways
236 (RCPs): CIMC5-RCP45 and CIMC5-RCP85, as well as four global circulation models
237 (GCMs): bbc-csm1-1, CESM1-BGC, HadGEM2-AO and MRI-CGCM3. These GCMs were
238 privileged based on their dissimilarity, according to the distance matrix calculated for all
239 available GCMs presented in Sanderson, Knutti, & Caldwell (2015). Future bioclimatic
240 predictions for each variable of interest were then downloaded from CHELSA V1.2 for
241 every scenario at two dates, 2050 and 2070, and later cropped to fit the study area. Because
242 dispersal is considered here as a key factor to constrain future species distributions, the
243 bioclimatic data was interpolated by decade to provide frequent steps to include dispersal
244 limitations (Engler et al. 2012). To do so, simple linear regressions were used to obtain for
245 each bioclimatic variables the 2010, 2020, 2030 and 2040 values using a coefficient
246 calculated for the 2000-2050 period following a similar procedure to the one employed by
247 Adhikari et al. (2018). The same procedure was applied for 2060 based on the 2050-2070
248 period, and for decades 2080, 2090 and 2100, values by extrapolating the 2050-2070
249 regression coefficient into the future. All statistical analyses were conducted in R 4.3.1 (R
250 Core Team, 2019).

251 Dispersal capacity

252 The widely-used *dispeRsal* function developed by Tamme et al. (2014) was chosen to
253 estimate dispersal capacity in form of maximum dispersal distance, which is usually more
254 suitable to include in SDMs than mean distance (Vittoz, & Engler, 2007; Thomson et al.
255 2011). Beforehand, a basic trait database including plant height, vegetation stratum, main
256 dispersion mode and seed mass was compiled for the 435 species. For plant height and
257 vegetation stratum, information at the species level was retrieved from online herbarium
258 material, such as the Field Museum (<https://plantidtools.fieldmuseum.org>), COL herbarium
259 (www.biovirtual.unal.edu.co) and Plant JSTOR (<https://plants.jstor.org>), directly measured
260 and averaged using at least four specimens per species when available. Dispersion mode and
261 seed mass data at the species level were usually unavailable and therefore, information
262 provided at the genus level from the Kew Botanical Garden seed collection initiative
263 (<http://data.kew.org/sid>), and specific páramo literature were used (Frantzen, & Bouman,
264 1989; Melcher, Bouman, & Cleef, 2000, 2004). Assuming for simplicity reasons that species
265 would disperse only once yearly, the *dispeRsal* function was run as a kernel-shape
266 probability density function of dispersal distances to calculate maximum dispersal distances
267 (in m/yr) (Tamme et al. 2014; Bullock et al. 2017). The raw results were then upscaled to
268 km per decade to fit the future bioclimatic predictions. Finally, dispersal capacity of mid-
269 páramo and super-páramo species were sommelly compared by means of a t-Student test.

270 Species distribution models

271 The current distribution of each species was modelled based on actual environmental
272 conditions, represented by the 5 bioclimatic variables selected, and dispersal capacity. The
273 latter factor was introduced as a new variable, set by log-transforming the species maximum
274 dispersal distance previously computed from plant traits and scaling the obtained values
275 between 0 and 1 to rank species from bad to good dispersers (function *iForce*, *iSDM*
276 package; Hattab et al. 2017). SDMs were then run using two different families of algorithms
277 fitted for presence-absence data: i) generalized linear models (GLMs), which explore the
278 linear relationship between explanatory and explained variables through a flexible Gaussian-
279 identity distribution-link approach and were fitted using second degree polynomial curves
280 and ii) random forests (RFs) that integrate the data through an ensemble learning, coupling
281 decision trees with classification and regression settings/approaches (*biomod2* package;
282 Thuiller et al. 2016). For each species, the data was divided into a 75% training dataset and
283 a 25% testing dataset, and run with 50 models per algorithm. The true skill statistic (TSS)

284 value was computed for each model to evaluate SDMs' performances and all models with a
285 TSS value greater than 0.6, either obtained with the GLM or RF algorithms, were retained
286 (Allouche, Tsoar, & Kadmon, 2006). The final models were then ensembled to obtain the
287 final probabilistic predictions (Araújo, & New, 2007; Marmion, Parviainen, Luoto,
288 Heikkinen, & Thuiller, 2009), which were finally transformed into binary values using a
289 threshold approach that equalizes the sensitivity and specificity metrics (*optimal.threshold*
290 *function*; *ecospat* package; Liu, Berry, Dawson, & Pearson, 2005; Di Cola et al. 2017).

291 The calibrated current models were then used to project species' distributions into
292 the future per decade and under each of the 8 different climate-change scenarios. To do so,
293 the previously-used dispersal covariate was set to 0 and future distributions were projected
294 against bioclimatic predictors only, in order to alleviate the static species-specific dispersal
295 constraint. As formerly done, the probabilistic projections for each decade were then
296 transformed into binary values and constrained in temporal order by the species maximum
297 dispersal distance (Engler et al. 2012), hence allowing to track progressive changes in
298 species distributions depending on available bioclimatic conditions and capacity to disperse
299 from the previous distribution. Additional biogeographical barriers represented by the
300 Andean forest and anthropogenic activities from the lowlands were also considered by using
301 a raster mask at each time step that assumed that all pixels below the 3000 m isohypse were
302 unsuitable. Thus, a species could only cross the matrix of unsuitable conditions in a time-
303 step if its maximum dispersal distance was greater than the distance separating two suitable
304 pixels. The set of decadal binary maps obtained for each species separately offered time
305 series of species redistribution that can be used to assess the species-specific proportion of
306 areas that were lost, gained or that remained occupied by the focal species between present
307 and 2100 (functions *migclim.distance* and *migclim.plot*, *migclim* package; Engler et al.
308 2012). Finally, the 2100 binary prediction was used to fit the 2100 probabilistic prediction
309 for richness capacity (see below).

310 Changes in species distribution for the 21st century were evaluated as a binary result,
311 net loss or net gain, by comparing and quantifying the number of pixels belonging to the
312 2000 and 2100 distributions. Finally, extinction risk was considered when a species had at
313 least one scenario predicting its complete extinction (i.e. the species completely disappeared
314 from the studied area) by 2100. The severity of the risk was evaluated based on the number
315 of scenarios predicting extinction by 2100, i) low risk (1-2 scenarios), ii) intermediate risk
316 (3-4 scenarios), high risk (5-6 scenarios) and extinct (7-8 scenarios).

317

318 Model richness and assemblages

319 The SESAM framework relies on the *predict first assemble later* principle (Guisan, &
320 Rahbek, 2011), meaning that final community predictions are achieved after applying an
321 assembly procedure that consists in selecting species from the predicted pool until reaching
322 the carrying capacity of a community defined as potential richness (Guisan, & Rahbek, 2011;
323 Mateo et al. 2017). This local carrying capacity (at pixel level) is often estimated by either
324 stacking the probabilities predicted by the SDMs or by using macroecological models
325 (D'Amen et al. 2015a; Mateo et al. 2017) but the former has the advantage of being
326 embedded within a same S-SDM framework and allowing for a varying timeline, so that we
327 used it here. All SDMs in their probabilistic form were stacked in 2000 and 2100 for each
328 scenario to evaluate richness. Net richness change at the pixel level was assessed as a
329 percentage of the current (2000) richness, with positive and negative values meaning a net
330 gain and loss, respectively, in potential species richness.

331 Finally, species composition at the pixel level was predicted through the probability
332 ranking rule (PRR; D'Amen et al. 2015b), which consists in selecting species from the
333 predicted pool in decreasing order of their SDM probability of occurrence until reaching the
334 previously predicted potential richness. The PRR was applied to the stacks of SDM
335 predictions for 2000 and 2100 using the *prc.ecospat* function of the *ecospat* package (Di
336 Cola et al. 2017). Changes in composition, expressed as numbers of species gained and lost,
337 as well as ratio of mid-páramo and super-páramo species to emulate upward migration and
338 high-elevation competition, were evaluated for the 10 main páramo sky islands. Lastly,
339 based on the estimated changes in richness and composition, local vulnerability to climate
340 change was assessed.

341 **Results**

342 Species varied greatly in terms of their maximum dispersal distance, ranging from 0.008 to
343 6027 m/yr in a negative exponential manner with a mean of 193 m/yr (\pm 647) (Fig. S2; Table
344 S2). Mid-páramo and super-páramo species showed significantly different maximum
345 dispersal distances (t-test: 4.2972, df: 423.26, p-value: 2.148e-05), with mid-páramo species
346 dispersing relatively well in average at 227.14 m/yr (\pm 714), while super-páramo species
347 showed shorter dispersal distances at 51.39 m/yr (\pm 136). Long dispersal distances were
348 usually associated with shrub genera with relatively heavy seeds (10-100 mg) and using
349 zoochory or assisted anemochory, such as *Monnina* (Polygalaceae) and *Gaiadendron*

350 (Loranthaceae), whereas short dispersal distances was common in small herbaceous plants
351 with lightweight seeds (0.0001-0.001 mg) and using unassisted anemochory or autochory as
352 principal dispersal mode, as seen in *Aa* (Orchidaceae) and *Ourisia* (Plantaginaceae).

353 The performance of SDMs varied between species, and the average values were
354 considered acceptable overall (across models: mean TSS = 0.614, Sensitivity = 79.835,
355 Specificity = 78.952; Table 1). In general, the RF algorithm performed better than the GLM
356 algorithm, and more of its models were retained, approximately 29% across all species.
357 About 70% of the SDMs across all scenarios predicted a net loss in species' spatial
358 distribution and only 30% predicted a net gain (Fig. 2). A total of 65 species (15% of all
359 species) presented a degree of extinction risk under at least one scenario by the end of the
360 century, 18 of which as a low risk, eight as an intermediate risk, 15 as a high risk and finally
361 39 were predicted to become totally extinct from the studied area by 2100. The most
362 endangered genera encountered in numbers were *Cerastium* (3 species), *Draba* (3 species),
363 *Gentianella* (4 species) and *Viola* (3 species). In addition, 22 of the 65 species were super-
364 páramo species, 5 of which are known endemics at the national scale: *Aetheolaena*
365 *involutrata*, *Bartsia pumila*, *Festuca chimborazensis*, *Loricaria artisanensis* and *Viola*
366 *polycephala*. Finally, of the 39 species with the highest extinction risk, 10 were super-
367 páramo species known as páramo endemics, for example *Cerastium candicans*, *Draba*
368 *depressa*, *Lachemilla tanacetifolia*, *Lupinus alopecuroides* and *Xenophyllum crassum*.

369 Regarding net richness changes in the páramo sky islands, the general trend at pixel
370 level (alpha diversity) was a loss of 56.63 % (± 20.83) of the original species richness
371 between the present and 2100 (Fig. 3). The most affected areas were the northern mountains
372 of Pichincha and Ilinizas with an average loss of 82.64 (± 2.15) and 77.24% (± 3.95)
373 respectively. Contrarily, the least affected areas were the central mountains of Tungurahua
374 and Altar with an average loss of 13.52 % (± 11.12) and 31.90 % (± 6.52) respectively, and
375 punctual pixels with positive values hence gaining species, up to 18.73 % on the
376 Chimborazo.

377 At the sky island level, important significant composition changes in the final plant
378 communities were observed (Fig. 3; Fig S3; Table S3). Sky islands lost an average 64.74%
379 (± 14.12) of their original species pool (gamma diversity), Pichincha and Ilinizas being the
380 most significantly affected with losses of 85.68% (± 5.70) and 74.73% (± 5.12) respectively.
381 By contrast, Altar and Tungurahua were the least affected, losing 46.49 (± 10.76) and

382 50.00% (± 9.74) respectively. Gains at this scale did not compensate losses, with the average
383 gain reaching 12.97 % (± 11.41), some páramos gaining more species such as Tungurahua
384 and Altar with 39.21% (± 5.03) and 20.86% (± 6.31), while others gained less, such as
385 Cayambe and Antisana with 7.17 % (± 3.02) and 7.47 % (± 3.05). The most drastic changes
386 were therefore observed for the northern mountains of Cayambe and Pichincha.

387 On average in 2000, the ratio between mid-páramo and super-páramo species in the
388 páramo sky islands reached 68.79 / 31.21 (± 6.09), and changed across all scenarios in 2100
389 to 73.61 / 26.39 (± 4.46), meaning that approximately 4.82% of super-páramo species were
390 replaced with mid-páramo ones (Table 2). The most drastic tendencies were observed for
391 Ilinizas and Antisana, losing 9.76 and 8.01% of their super-páramo species respectively,
392 while the least affected sky islands were Cayambe, which gained 0.78% of super-paramo
393 species, and Sangay that lost 0.48% of super-paramo species. Based on richness at pixel and
394 sky island level and composition changes, Ilinizas, Pichincha and in lesser means Antisana
395 were therefore considered as most threatened by climate change.

396 **Discussion**

397 Mountains are particularly sensitive to climate change because they are often prone to
398 accelerated changes and more rapid responses of biota in comparison with lowlands
399 (Bertrand et al. 2011; Smith, Edmonds, Hartin, Mundra, & Calvin, 2015; Steinbauer et al.
400 2018). Neotropical mountains in particular are classified as *highly vulnerable* to climate
401 change (Team et al. 2014) and are expected to suffer drastic changes in biodiversity and its
402 associated ecosystem services that will affect millions of people on the short to mid-term
403 (Buytaert et al. 2011; Tovar et al. 2013; Anthelme, & Lavergne, 2018). In addition, the fast
404 and important changes in rural occupation and land uses that are occurring due to improving
405 socio-economic conditions and the subsequent population growth, contribute greatly to the
406 extent and intensity of environmental degradation (Hofstede, Segarra, & Vásconez, 2003).
407 It is also in this region that predicting the impacts of future global changes becomes
408 particularly challenging, due to data availability and the lack of knowledge on biodiversity,
409 climatic variations, anthropogenic dynamics and the responses of biodiversity to these
410 drivers (Anderson et al. 2011; Ramírez-Villegas et al. 2014; Lenoir, & Svenning 2015;
411 Feeley et al. 2017).

412 Dispersal capacity

413 To date, trait data and functional analyses for the páramo remain scarce, especially regarding
414 non-leaf characteristics (e.g. Sánchez et al. 2014), and so far few works have focused on
415 seed-related traits and characterized the dispersal modes of páramo species (Frantzen, &
416 Bouman, 1989; Melcher et al. 2000; Melcher et al. 2004). Our estimates of species maximum
417 dispersal distances based on plant dispersal traits highlighted that páramo species disperse
418 on the lower end of the terrestrial angiosperm dispersal spectrum (Kinlan, & Gaines, 2003)
419 and in general similarly to other alpine floras (Vittoz, & Engler, 2007; Morgan, & Venn,
420 2017). Our result showed some support for the hypothesis that low-elevation shrubs,
421 characterized by heavy seeds and usually using either zoochory (e.g. Ericaceae) or assisted
422 anemochory (e.g. Asteraceae), disperse best. Indeed, the correlation favouring plant height
423 over seed mass seemed particularly advantageous for these shrub species, at least at the
424 landscape level (Parolo, & Rossi, 2008; Thomson et al. 2011, 17), whereas within a same
425 dispersal syndrome or vegetation type, light-seed species that disperse anemochorously are
426 usually considered as more efficient (Muller-Landau et al. 2008). Our best dispersers were
427 often zoochorous and presenting relatively large fruits visible to vertebrate animals, such as
428 birds, which undoubtedly enhanced local dispersal (Thomson et al. 2011; Tamme et al. 2014)
429 and also increased frequency of long-distance dispersal events, for example between
430 mountain tops (Vittoz et al. 2009). Consequently, an upcoming challenge for these plant
431 species in the future is facing their own responses to climate change but also those of their
432 animal disperser (Travis et al. 2013). With increasing elevation and distance from the
433 treeline, Poaceae become progressively dominant in the páramo ecosystems, ensuing a larger
434 proportion of anemochorous species that often present dispersal-enhancing structures, i.e.
435 wings or pappi. Such structures are also crucial in helping plants overcome the long-distance
436 dispersal limitations they face in alpine areas (Vittoz et al. 2009; Morgan, & Venn, 2017;
437 Thomson et al. 2017). In the super-páramo belt, small characteristic plants such as
438 *Nototriche*, *Draba* and *Ourisia* (Peyre et al. 2018) are often featuring perennality, small
439 light-seeds, high autogamy rate and little seed productivity, which might explain the short-
440 distance dispersal tendency observed. In addition, the yet inhospitable environment and
441 unavailability of efficient animal dispersers on these sky-islands often forces plant species
442 to recur to vegetative (clonal) reproduction in priority and limit their sexual reproduction
443 (Vittoz et al. 2009). Accounting for establishment capacity, the availability of microsites,
444 good microclimatic and edaphic conditions, and strong species interactions, such as
445 facilitation of assisted dispersal, is therefore key to finally assess the migration capacity of
446 these species (Scherrer, & Körner, 2011; Anthelme, Cavieres, & Dangles, 2014; Hupp,

447 Llambí, Ramírez, & Callaway, 2017; Alexander et al. 2018). Finally, considering the
448 competitiveness of super-páramo species against advantaged shrub and herbaceous species
449 from lower elevations, including opportunistic and exotic species, is necessary to evaluate
450 the intensity of the threat (Pauchard et al. 2009; Llambí, Hupp, Saez, & Callaway, 2018).

451 The importance of dispersal capacity in shaping a species distribution has long been
452 acknowledged and increasingly included to improve SDM performances in the last decade
453 (Thuiller et al. 2008; Dullinger et al. 2012; Bateman et al. 2013; Hattab et al. 2017).
454 Community modelling has been considerably improving in parallel, with considerable
455 efforts being put on better accounting for community assembly processes, including the
456 carrying capacity of communities and assembly rules (D'Amen et al. 2017; Mateo et al.
457 2017), nonetheless, dispersal constraints had remained mostly overlooked in community
458 modelling (D'Amen et al. 2017; Guisan et al. 2019). This study supports that dispersal is a
459 key factor in defining the future distribution of species and their assemblages, as illustrated
460 in Fig. 2 by the overall overprediction of potential versus realized distributions quantified as
461 the *suitable but unoccupied area*. Our finding is therefore in agreement with previous works
462 maintaining that dispersal capacity is particularly important in tropical mountains, where
463 climate has had an important but not exclusively prevailing influence on biota distribution
464 (e.g. Flantua, O'dea, Onstein, Giraldo, & Hooghiemstra, 2019). Our results also suggest that
465 super-páramo plants might not be able to migrate altitudinally along the same mountain but
466 also be prevented in their attempts to colonize new mountain ranges, sustaining the key role
467 of topographic distance and isolation (Sklenář, & Jørgensen, 1999; Flantua et al. 2019).

468 Distribution responses of plant species

469 Of all species, 70% were predicted to show a significant distribution loss by 2100, which
470 complements previous findings in which 50-60% of tropical Andean species reduced their
471 distribution in the second half of the 21st century (Ramírez-Villegas et al. 2014). Even more
472 concerning is that 15% of all páramo species showed a significant extinction risk by 2100,
473 and 25% of all super-páramo species, supporting our hypothesis that super-páramo species
474 are generally more at risk than mid-páramo ones. Among the vulnerable super-páramo
475 species are several diagnostic species of super-páramo phytogeographical units, for example
476 *Ourisia muscosa* of the *Upper humid super-páramo* and *Draba depressa* of the *Upper dry*
477 *super-páramo* (Peyre et al. 2018). Furthermore, our results posed as threatened many super-
478 páramo species that are páramo endemics such as *Cerastium candicans*, *Draba depressa* and
479 *Xenophyllum crassum* or even national páramo endemics, for example *Bartsia pumila*,

480 *Loricaria antisanensis* and *Viola polycephala*. Our study alerts of maximum extinction risk
481 for 9% of all studied species, some of which were already classified following the IUCN
482 system as threatened, for example *Bartsia pumila* (VU) and *Gentianella hirculus* (EN), but
483 also some considered as not threatened, such as *Gentianella limoselloides* (LC) and *Halenia*
484 *taruga-gasso* (NT) (León-Yáñez, 2012). Because SDMs can be a useful complement to
485 further conduct UICN evaluations (Breiner, Guisan, Nobis, & Bergamini, 2017; but see
486 Akcakaya, Butchart, Mace, Stuart, & Hilton-Taylor, 2006), we therefore urge, based on the
487 SDM results to focus further study on these predicted-extinct species, especially regarding
488 population health and individual fitness, and encourage ex-situ conservation efforts such as
489 seed banks to preserve this unique biodiversity.

490 Changes in richness and plant assemblages

491 Local richness at the pixel level has been found to significantly decrease in most sky islands,
492 even accounting for potential colonization from lower elevations. The northern sky islands
493 of Ilinizas and Pichincha were the most affected, which contradicts previous findings stating
494 richness stability in this region (Ramírez-Villegas et al. 2014), and exceptions to the rule
495 included few central mountains such as Tungurahua and Altar where richness would remain
496 stable or even increase slightly. As a result, these last sky islands might be experiencing the
497 worldwide-observed *accelerated colonization process* on mountains (Steinbauer et al.
498 2018), but buffered by specific environmental conditions and a particularly vulnerable
499 species pool. Overall, we found no support for the negative relationship hypothesis between
500 actual richness and future richness changes, as the more diverse (at the local scale, or plot
501 scale) eastern mountains suffered less drastic changes than the less diverse northern
502 mountains (Peyre et al. 2019). Because this finding plausibly supposes that the communities'
503 richness capacity is not reached on these sky islands, we recommend further scientific focus
504 on that particular macroecological hypothesis.

505 Composition changes were also predicted as very abrupt in the region, estimating
506 important species losses and little gains at the sky island level (gamma diversity). Northern
507 mountains were predicted to lose substantial amounts of species as much as 85% in
508 Pichincha and gain very few species overall. By contrast, central mountains saw moderate
509 losses and in the case of Tungurahua, a potential even loss and gain, depending on the
510 climate change scenario considered. Several complementary hypotheses to climate change
511 might be advanced to explain such a pattern, for example the geographic isolation and
512 elevation of the massif, which could either facilitate or constrain dispersal and migration

513 (Sklenář, & Jørgensen, 1999). Finally, the ratio of super-páramo vs. mid-páramo species
514 decreased by 2100, especially in northern mountains, sky islands generally losing 5% of
515 their super-páramo species to mid-páramo ones. Our results therefore support previous
516 findings that mid-páramo species are moving upslope and competing with super-páramo
517 species, although the role of adaptation, microenvironmental refugia and biotic interactions
518 remain to be considered for more refined plant responses.

519 Our results evidenced that sky islands from northern Ecuador, including Pichincha
520 and Ilinizas, were evaluated as the most vulnerable to future climate change. These páramos
521 are located along the inter-Andean valley where an important population resides, i.e. Quito
522 and Latacunga, making the anthropogenic change expected for the end of the century in the
523 form of fast and intense land-use changes an even bigger threat than climate change
524 (Hofstede et al. 2003). Because the agricultural frontier could move upslope too when soil
525 develops sufficiently at high altitude, entire super-páramo ecosystems could suffer drastic
526 changes in their structure and functions. Therefore, the predictions provided here, based on
527 climate-change solely, should be considered as conservative scenarios and even more
528 forceful impacts should be expected under a global change scenario. In addition, exotic and
529 efficiently dispersed opportunistic species could take advantage of the anthropogenic change
530 to migrate and invade the sky islands, competing directly with local species and forming no-
531 analog communities with little ecological value (Le Roux, & McGeoch, 2008; Anthelme, &
532 Peyre, 2019). Precise monitoring should therefore be tracking the anthropogenic changes
533 associated to climate change on these sky islands in priority so to prevent a critical threat to
534 the sky islands of the northern Andes currently holding the reservoir or museum of super-
535 páramo species.

536 Study limitations and future recommendations

537 Regarding dispersal estimates, we consider that even though trait-based dispersal distance
538 methods such as Tamme et al. (2014) are very useful and give reasonable predictions, the
539 fact that they have been shown to underestimate distances for wind-dispersed species, an
540 important proportion of our species pool (Herrmann et al. 2016, Morgan, & Venn, 2017),
541 would support the use of more detailed techniques in the future, for example mechanistic
542 models that acknowledge wind velocities and dispersal pathways (Skarpaas et al. 2004;
543 Holloway et al. 2016). Moreover, we did not account for certain crucial variation such as i)
544 potential changes in biogeographical barriers with climate change such as glacier retreat or

545 forest expansion, which might affect the dispersal reach of species (Caplat et al. 2016), nor
546 did we consider ii) that specific dispersal distances might change over time (Travis et al.
547 2013) or iii) the importance of long dispersal events promoted by climate change
548 consequences such as the frequency and intensity of storms (Hellmann, Byers, Bierwagen,
549 & Dukes, 2008). Another limitation regards data availability and coverage, a commonly
550 encountered issue in tropical research. In fact, the species list was recovered from
551 VegParamo, which is a pioneer database with important representativity of the páramo taxa,
552 although it still accounts for certain geographic and taxonomic knowledge gaps (Peyre et al.
553 2015; Bottin et al. 2019). Finally, climatic interpolations in tropical mountain areas that are
554 topographically and environmentally complex are particularly challenging to obtain,
555 especially for a broad study area and future climatic scenarios, and more fitted climatic data
556 with a finer resolution could have improved the models performance and predictions.

557 Future recommendations include complementing the trait data with observed data and
558 calculate distance on site to provide better estimates of dispersal capacity of plants in the
559 region. To improve the models' accuracy and ecological meaning, it would be useful to
560 account for different dynamic factors unavailable at the time (Anthelme et al. 2014; Graae
561 et al. 2018), for example: i) additional abiotic variables at the macroscale, such as horizontal
562 precipitation that represents an important water intake for plants, but also meso and
563 microscale, for example local night freezing, that could balance macroeffects (Scherrer, &
564 Körner, 2011; Mod et al. 2015), ii) fine biotic interactions to incorporate into the assembly
565 rules, competition but also facilitation to dispersal or establishment (Llambí et al. 2018), and
566 iii) land-use changes, whose intensity and expansion might increase under future climate
567 change (Hofstede et al. 2003; Anderson et al. 2011).

568 **Acknowledgements**

569 We thank Dr. Fabien Anthelme for revising the final form of the paper.

570 **Author contributions**

571 G.P. and A.G. conceived of the research idea; G.P., M.G. and A.G. processed the data;

572 G.P. performed the statistical analyses and wrote the paper; all authors discussed the

573 methods, results and commented on the manuscript.

574 **Data accessibility**

575 The vegetation data is freely available from VegParamo (www.vegparamo.com), and on

576 Dryad (<https://datadryad.org/>; Peyre, 2020).

577 **References**

- 578 Adhikari, P., Shin, M. S., Jeon, J. Y., Kim, H. W., Hong, S., & Seo, C. (2018). Potential
579 impact of climate change on the species richness of subalpine plant species in the mountain
580 national parks of South Korea. *Journal of Ecology and Environment*, 42(1), 36.
581 <https://doi.org/10.1186/s41610-018-0095-y>
- 582 Akcakaya, H. R., Butchart, S. H. M., Mace, G. M., Stuart, S. N., & Hilton-Taylor, C. (2006).
583 Use and misuse of the IUCN Red List Criteria in projecting climate change impacts on
584 biodiversity. *Global Change Biology*, 12, 2037–2043. <https://doi.org/10.1111/j.1365-2486.2006.01253.x>
- 586 Alexander, J. M., Chalmandrier, L., Lenoir, J., Burgess, T. I., Essl, F., Haider, S., ... &
587 Pauchard, A. (2018). Lags in the response of mountain plant communities to climate change.
588 *Global change biology*, 24(2), 563–579. <https://doi.org/10.1111/gcb.13976>
- 589 Allouche, O., Tsoar, A. & Kadmon, R. (2006). Assessing the accuracy of species distribution
590 models: prevalence, kappa and the true skill statistic (TSS). *Journal of Applied Ecology*, 43,
591 1223–1232. <https://doi.org/10.1111/j.1365-2664.2006.01214.x>
- 592 Anderson, E. P., Marengo, J., Villalba, R., Halloy, S., Young, B., Cordero, D., ... & Martinez,
593 R. (2011). *Consequences of climate change for ecosystems and ecosystem services in the*
594 *tropical Andes*. In S. K. Herzog, R. Martínez, P. M. Jørgensen & H. Tiessen (Eds.) *Climate*
595 *Change and Biodiversity in the Tropical Andes* (pp. 1–18). São José dos Campos, Brazil:
596 Inter-American Institute for Global Change Research (IAI) and Scientific Committee on
597 Problems of the Environment (SCOPE)
- 598 Anthelme, F., Cavieres, L. A., & Dangles, O. (2014). Facilitation among plants in alpine
599 environments in the face of climate change. *Frontiers in plant science*, 5, 387.
600 <https://doi.org/10.3389/fpls.2014.00387>
- 601 Anthelme, F., & Lavergne, S. (2018). Alpine and arctic plant communities: a worldwide
602 perspective. *Perspectives in Plant Ecology Evolution and Systematics*, 30, 1–5. <https://doi.org/10.1016/j.ppees.2017.12.002>
- 604 Anthelme, F., & Peyre, G. (2019). *Biogeography of South American Highlands*. Reference
605 Module in Earth Systems and Environmental Sciences, Encyclopedia of the World's biomes,
606 Elsevier. <https://doi.org/10.1016/B978-0-12-409548-9.11811-1>.
- 607 Araújo, M. B., & Guisan, A. (2006). Five (or so) challenges for species distribution
608 modelling. *Journal of biogeography*, 33(10), 1677–1688. <https://doi.org/10.1111/j.1365-2699.2006.01584.x>
- 610 Araújo, M.B., Thuiller, W. & Pearson, R.G. (2006) Climate warming and the decline of
611 amphibians and reptiles in Europe. *Journal of Biogeography*, 33, 1712–1728.
612 <https://doi.org/10.1111/j.1365-2699.2006.01482.x>
- 613 Araújo, M. B., & New, M. (2007). Ensemble forecasting of species distributions. *Trends in*
614 *Ecology & Evolution*, 22, 42–47. <https://doi.org/10.1016/j.tree.2006.09.010>
- 615 Araújo, M. B., Anderson, R. P., Barbosa, A. M., Beale, C. M., Dormann, C. F., Early, R., ...
616 & Rahbek, C. (2019). Standards for distribution models in biodiversity assessments. *Science*
617 *Advances*, 5, eaat4858. <https://doi.org/10.1126/sciadv.aat4858>

- 618 Bateman, B. L., Murphy, H. T., Reside, A. E., Mokany, K., & VanDerWal, J. (2013).
619 Appropriateness of full-, partial-and no-dispersal scenarios in climate change impact
620 modelling. *Diversity and Distributions*, 19(10), 1224–1234.
621 <https://doi.org/10.1111/ddi.12107>
- 622 Bertrand, R., Lenoir, J., Piedallu, C., Riofrío-Dillon, G., de Ruffray, P., Vidal, C., ... &
623 Gégout, J. C. (2011). Changes in plant community composition lag behind climate warming
624 in lowland forests. *Nature*, 479, 517. <https://doi.org/10.1038/nature10548>
- 625 Bottin, M., Peyre, G., Vargas, C., Raz, L., Richardson, J. E., & Sanchez, A. (2019).
626 Phytosociological data and herbarium collections show congruent large-scale patterns but
627 differ in their local descriptions of community composition. *Journal of Vegetation Science*,
628 31(1), 208–219. <https://doi.org/10.1111/jvs.12825>
- 629 Braun-Blanquet, J. (1964). *Pflanzensoziologie: Grundzüge der Vegetationskunde*. New
630 York, NY, US: Springer.
- 631 Breiner, F. T., Guisan, A., Nobis, M. P., & Bergamini, A. (2017). Including environmental
632 niche information to improve IUCN Red List assessments. *Diversity and Distributions*, 23,
633 484–495. <https://doi.org/10.1111/ddi.12545>
- 634 Bullock, J. M., Mallada González, L., Tamme, R., Götzenberger, L., White, S. M., Pärtel,
635 M., & Hooftman, D. A. (2017). A synthesis of empirical plant dispersal kernels. *Journal of*
636 *Ecology*, 105, 6–19. <https://doi.org/10.1111/1365-2745.12666>
- 637 Buytaert, W., Cuesta-Camacho, F., & Tobón, C. (2011). Potential impacts of climate change
638 on the environmental services of humid tropical alpine regions. *Global Ecology and*
639 *Biogeography*, 20, 19–33. <https://doi.org/10.1111/j.1466-8238.2010.00585.x>
- 640 Caplat, P., Edelaar, P., Dudaniec, R. Y., Green, A. J., Okamura, B., Cote, J., ... & Petit, E. J.
641 (2016). Looking beyond the mountain: dispersal barriers in a changing world. *Frontiers in*
642 *Ecology and the Environment*, 14(5), 261–268. <https://doi.org/10.1002/fee.1280>
- 643 Chen, S. C., Tamme, R., Thomson, F. J., & Moles, A. T. (2019). Seeds tend to disperse
644 further in the tropics. *Ecology letters*, 22(6), 954–961. <https://doi.org/10.1111/ele.13255>
- 645 Cuatrecasas, J. (1958). Aspectos de la vegetación natural de Colombia. *Revista de la*
646 *Academia Colombiana de Ciencias Exactas, Físicas y Naturales*, 10, 221–268.
- 647 Cuesta, F., Llambí, L. D., Huggel, C., Drenkhan, F., Gosling, W. D., Muriel, P., ... & Tovar,
648 C. (2019). New land in the Neotropics: a review of biotic community, ecosystem, and
649 landscape transformations in the face of climate and glacier change. *Regional environmental*
650 *change*, 1–20. <https://doi.org/10.1007/s10113-019-01499-3>
- 651 D'Amen, M., Dubuis, A., Fernandes, R. F., Pottier, J., Pellissier, L., & Guisan, A. (2015a).
652 Using species richness and functional traits predictions to constrain assemblage predictions
653 from stacked species distribution models. *Journal of Biogeography*, 42, 1255–1266.
654 <https://doi.org/10.1111/jbi.12485>
- 655 D'Amen, M., Pradervand, J. N., & Guisan, A. (2015b). Predicting richness and composition
656 in mountain insect communities at high resolution: a new test of the SESAM framework.
657 *Global Ecology and Biogeography*, 24, 1443–1453. <https://doi.org/10.1111/geb.12357>

- 658 D'Amen, M., Rahbek, C., Zimmermann, N. E., & Guisan, A. (2017). Spatial predictions at
659 the community level: from current approaches to future frameworks. *Biological Reviews*,
660 92, 169–187. <https://doi.org/10.1111/brv.12222>
- 661 Di Cola, V., Broennimann, O., Petitpierre, B., Breiner, F. T., D'amen, M., Randin, C., ... &
662 Guisan, A. (2017). ecospat: a R package to support spatial analyses and modeling of species
663 niches and distributions. *Ecography*, 40, 774–787. <https://doi.org/10.1111/ecog.02671>
- 664 Diaz, S., Settele, J., Brondízio, E., Ngo, H., Guèze, M., Agard, J., ... & Chan, K. (2019).
665 *Summary for policymakers of the global assessment report on biodiversity and ecosystem*
666 *services of the Intergovernmental Science-Policy Platform on Biodiversity and Ecosystem*
667 *Services*.
- 668 Dirnböck, T., & Dullinger, S. (2004). Habitat distribution models, spatial autocorrelation,
669 functional traits and dispersal capacity of alpine plant species. *Journal of Vegetation Science*,
670 15(1), 77–84. <https://doi.org/10.1111/j.1654-1103.2004.tb02239.x>
- 671 Dormann, C. F., Elith, J., Bacher, S., Buchmann, C., Carl, G., Carré, G., ... & Lautenbach,
672 S. (2013). Collinearity: a review of methods to deal with it and a simulation study evaluating
673 their performance. *Ecography*, 36, 27–46. [https://doi.org/10.1111/j.1600-](https://doi.org/10.1111/j.1600-0587.2012.07348.x)
674 [0587.2012.07348.x](https://doi.org/10.1111/j.1600-0587.2012.07348.x)
- 675 Dullinger, S., Gattlinger, A., Thuiller, W., Moser, D., Zimmermann, N. E., Guisan, A., . . .
676 Hülber, K. (2012). Extinction debt of high-mountain plants under twenty-first-century
677 climate change. *Nature Climate Change*, 2, 619–622. <https://doi.org/10.1038/nclimate1514>
- 678 Engler, R., Hordijk, W., & Guisan, A. (2012). The MIGCLIM R package—seamless
679 integration of dispersal constraints into projections of species distribution models.
680 *Ecography*, 35, 872–878. <https://doi.org/10.1111/j.1600-0587.2012.07608.x>
- 681 Feeley, K. J., Stroud, J. T., & Perez, T. M. (2017). Most ‘global’ reviews of species’
682 responses to climate change are not truly global. *Diversity and Distributions*, 23, 231–234.
683 <https://doi.org/10.1111/ddi.12517>
- 684 Flantua, S. G., O’dea, A., Onstein, R. E., Giraldo, C., & Hooghiemstra, H. (2019). The
685 flickering connectivity system of the north Andean páramos. *Journal of Biogeography*.
686 <https://doi.org/10.1111/jbi.13607>
- 687 Frantzen, N. M. L. H. F., & Bouman, F. (1989). Dispersal and growth form patterns of some
688 zonal páramo vegetation types. *Acta botanica neerlandica*, 38, 449–465.
689 <https://doi.org/10.1111/j.1438-8677.1989.tb01376.x>
- 690 Graae, B. J., Vandvik, V., Armbruster, W. S., Eiserhardt, W. L., Svenning, J. C., Hylander,
691 K., ... & Lenoir, J. (2018). Stay or go—how topographic complexity influences alpine plant
692 population and community responses to climate change. *Perspectives in Plant Ecology,*
693 *Evolution and Systematics*, 30, 41–50. <https://doi.org/10.1016/j.ppees.2017.09.008>
- 694 Guisan, A., & Thuiller, W. (2005). Predicting species distribution: offering more than simple
695 habitat models. *Ecology letters*, 8(9), 993–1009. [https://doi.org/10.1111/j.1461-](https://doi.org/10.1111/j.1461-0248.2005.00792.x)
696 [0248.2005.00792.x](https://doi.org/10.1111/j.1461-0248.2005.00792.x)
- 697 Guisan, A., & Rahbek, C. (2011). SESAM—a new framework integrating macroecological
698 and species distribution models for predicting spatio-temporal patterns of species

- 699 assemblages. *Journal of Biogeography*, 38(8), 1433–1444. <https://doi.org/10.1111/j.1365->
700 2699.2011.02550.x
- 701 Guisan, A., Mod, H. K., Scherrer, D., Münkemüller, T., Pottier, J., Alexander, J. M., &
702 D'Amen, M. (2019). Scaling the linkage between environmental niches and functional traits
703 for improved spatial predictions of biological communities. *Global Ecology and*
704 *Biogeography*. <https://doi.org/10.1111/geb.12967>
- 705 Hattab, T., Garzón-López, C. X., Ewald, M., Skowronek, S., Aerts, R., Horen, H., ... &
706 Lenoir, J. (2017). A unified framework to model the potential and realized distributions of
707 invasive species within the invaded range. *Diversity and Distributions*, 23, 806–819.
708 <https://doi.org/10.1111/ddi.12566>
- 709 Hellmann, J. J., Byers, J. E., Bierwagen, B. G., & Dukes, J. S. (2008). Five potential
710 consequences of climate change for invasive species. *Conservation biology*, 22(3), 534–543.
711 <https://doi.org/10.1111/j.1523-1739.2008.00951.x>
- 712 Herrmann, J. D., Carlo, T. A., Brudvig, L. A., Damschen, E. I., Haddad, N. M., Levey, D.
713 J., ... & Tewksbury, J. J. (2016). Connectivity from a different perspective: comparing seed
714 dispersal kernels in connected vs. unfragmented landscapes. *Ecology*, 97(5), 1274–1282.
715 <https://doi.org/10.1890/15-0734.1>
- 716 Hofstede, R., Segarra, P., & Vásconez, P. M. (2003). *Los páramos del mundo: Proyecto*
717 *Atlas Mundial de los Páramos*. Quito, Ecuador: UICN Global Peatland Initiative;
718 Ecociencia.
- 719 Holloway, P., Miller, J. A., & Gillings, S. (2016). Incorporating movement in species
720 distribution models: how do simulations of dispersal affect the accuracy and uncertainty of
721 projections?. *International Journal of Geographical Information Science*, 30(10), 2050–
722 2074. <https://doi.org/10.1080/13658816.2016.1158823>
- 723 Hupp, N., Llambí, L. D., Ramírez, L., & Callaway, R. M. (2017). Alpine cushion plants have
724 species-specific effects on microhabitat and community structure in the tropical Andes.
725 *Journal of vegetation science*, 28, 928–938. <https://doi.org/10.1111/jvs.12553>
- 726 Kammer, P. M., Schöb, C., & Choler, P. (2007). Increasing species richness on mountain
727 summits: Upward migration due to anthropogenic climate change or re-colonisation? *Journal*
728 *of Vegetation Science*, 18, 301–306. <https://doi.org/10.1111/j.1654-1103.2007.tb02541.x>
- 729 Karger, D. N., Conrad, O., Böhrer, J., Kawohl, T., Kreft, H., Soria-Auza, R. W., ... &
730 Kessler, M. (2017). Climatologies at high resolution for the earth's land surface areas.
731 *Scientific data*, 4, 170122. <https://doi.org/10.1038/sdata.2017.122>
- 732 Kinlan, B. P., & Gaines, S. D. (2003). Propagule dispersal in marine and terrestrial
733 environments: a community perspective. *Ecology*, 84(8), 2007–2020.
734 <https://doi.org/10.1890/01-0622>
- 735 Le Roux, P. C., & McGeoch, M. A. (2008). Rapid range expansion and community
736 reorganization in response to warming. *Global Change Biology*, 14, 2950–2962.
737 <https://doi.org/10.1111/j.1365-2486.2008.01687.x>
- 738 Lenoir, J., & Svenning, J. C. (2015). Climate-related range shifts—a global multidimensional
739 synthesis and new research directions. *Ecography*, 38, 15–28.
740 <https://doi.org/10.1111/ecog.00967>

- 741 León-Yáñez, S. (Ed.). (2012). *Libro rojo de las plantas endémicas del Ecuador*. Quito,
742 Ecuador: Herbario QCA, Pontificia Universidad Católica del Ecuador.
- 743 Liu, C.R., Berry, P.M., Dawson, T.P. & Pearson, R.G. (2005) Selecting thresholds of
744 occurrence in the 551 prediction of species distributions. *Ecography*, 28, 385–393.
745 <https://doi.org/10.1111/j.0906-7590.2005.03957.x>
- 746 Llambí, L. D., Hupp, N., Saez, A., & Callaway, R. (2018). Reciprocal interactions between
747 a facilitator, natives, and exotics in tropical alpine plant communities. *Perspectives in Plant*
748 *Ecology, Evolution and Systematics*, 30, 82–88. <https://doi.org/10.1016/j.ppees.2017.05.002>
- 749 Marmion, M., Parviainen, M., Luoto, M., Heikkinen, R. K., & Thuiller, W. (2009).
750 Evaluation of consensus methods in predictive species distribution modelling. *Diversity and*
751 *Distributions*, 15, 59–69. <https://doi.org/10.1111/j.1472-4642.2008.00491.x>
- 752 Mateo, R. G., Mokany, K., & Guisan, A. (2017). Biodiversity models: what if unsaturation
753 is the rule?. *Trends in ecology & evolution*, 32, 556–566.
754 <https://doi.org/10.1016/j.tree.2017.05.003>
- 755 Melcher, I. M., Bouman, F., & Cleef, A. M. (2000). Seed dispersal in páramo plants:
756 epizoochorous and hydrochorous taxa. *Plant Biology*, 2, 40–52. [https://doi.org/10.1055/s-](https://doi.org/10.1055/s-2000-9146)
757 2000-9146
- 758 Melcher, I. M., Bouman, F., & Cleef, A. M. (2004). Seed atlas of the monocotyledonous
759 genera of the páramo. *Flora-Morphology, Distribution, Functional Ecology of Plants*, 199,
760 286–308. <https://doi.org/10.1078/0367-2530-00157>
- 761 Mod, H. K., le Roux, P. C., Guisan, A., & Luoto, M. (2015). Biotic interactions boost spatial
762 models of species richness. *Ecography*, 38, 913–921. <https://doi.org/10.1111/ecog.01129>
- 763 Moles, A.T., Falster, D.S., Leishman, M.R. & Westoby, M. (2004) Small-seeded species
764 produce more seeds per square metre of canopy per year, but not per individual per lifetime.
765 *Journal of Ecology*, 92, 384–396. <https://doi.org/10.1111/j.0022-0477.2004.00880.x>
- 766 Morgan, J. W., & Venn, S. E. (2017). Alpine plant species have limited capacity for long-
767 distance seed dispersal. *Plant Ecology*, 218(7), 813–819. [https://doi.org/10.1007/s11258-](https://doi.org/10.1007/s11258-017-0731-0)
768 017-0731-0
- 769 Muller-Landau, H. C., Wright, S. J., Calderón, O., Condit, R., & Hubbell, S. P. (2008).
770 Interspecific variation in primary seed dispersal in a tropical forest. *Journal of Ecology*,
771 96(4), 653–667. <https://doi.org/10.1111/j.1365-2745.2008.01399.x>
- 772 Naimi, B., Hamm, N. A., Groen, T. A., Skidmore, A. K., & Toxopeus, A. G. (2014). Where
773 is positional uncertainty a problem for species distribution modelling?. *Ecography*, 37(2),
774 191–203. <https://doi.org/10.1111/j.1600-0587.2013.00205.x>
- 775 Panetta, A. M., Stanton, M. L., & Harte, J. (2018). Climate warming drives local extinction:
776 Evidence from observation and experimentation. *Science advances*, 4, eaaq1819.
777 <https://doi.org/10.1126/sciadv.aaq1819>
- 778 Parolo, G., & Rossi, G. (2008). Upward migration of vascular plants following a climate
779 warming trend in the Alps. *Basic and Applied Ecology*, 9(2), 100–107.
780 <https://doi.org/10.1016/j.baae.2007.01.005>

- 781 Pauchard, A., Kueffer, C., Dietz, H., Daehler, C. C., Alexander, J., Edwards, P. J., ... &
782 Seipel, T. (2009). Ain't no mountain high enough: plant invasions reaching new elevations.
783 *Frontiers in Ecology and the Environment*, 7, 479–486. <https://doi.org/10.1890/080072>
- 784 Pecl, G. T., Araújo, M. B., Bell, J. D., Blanchard, J., Bonebrake, T. C., Chen, I. C., ... &
785 Williams, S. E. (2017). Biodiversity redistribution under climate change: Impacts on
786 ecosystems and human well-being. *Science*, 355, eaai9214.
787 <https://doi.org/10.1126/science.aai9214>
- 788 Peyre, G. (2020). The fate of páramo plant assemblages in the sky islands of the northern
789 Andes - Table S1: Species presence-absence data. Dryad dataset.
790 <https://doi.org/10.5061/dryad.44j0zpc9z>
- 791 Peyre, G., Balslev, H., Martí, D., Sklenář, P., Ramsay, P., Lozano, P., ... & Font, X. (2015).
792 VegPáramo, a flora and vegetation database for the Andean páramo. *Phytocoenologia*, 45,
793 195–201. <https://doi.org/10.1127/phyto/2015/0045>
- 794 Peyre, G., Balslev, H., & Font, X. (2018). Phytoregionalisation of the Andean páramo.
795 *PeerJ*, 6, e4786. <https://doi.org/10.7717/peerj.4786>
- 796 Peyre, G., Balslev, H., Font, X., & Tello, J. S. (2019). Fine-scale plant richness mapping of
797 the Andean páramo according to macroclimate. *Frontiers in Ecology and Evolution*, 7, 377.
798 <https://doi.org/10.3389/fevo.2019.00377>
- 799 R Core Team (2019). R: A language and environment for statistical computing. R
800 Foundation for Statistical Computing, Vienna, Austria. URL <https://www.R-project.org/>.
- 801 Ramírez-Villegas, J., Cuesta, F., Devenish, C., Peralvo, M., Jarvis, A., & Arnillas, C. A.
802 (2014). Using species distributions models for designing conservation strategies of Tropical
803 Andean biodiversity under climate change. *Journal for Nature Conservation*, 22, 391–404.
804 <https://doi.org/10.1016/j.jnc.2014.03.007>
- 805 Sánchez, A., Posada, J. M., & Smith, W. K. (2014). Dynamic cloud regimes, incident
806 sunlight, and leaf temperatures in *Espeletia grandiflora* and *Chusquea tessellata*, two
807 representative species of the Andean Páramo, Colombia. *Arctic, Antarctic, and Alpine*
808 *Research*, 46, 371–378. <https://doi.org/10.1657/1938-4246-46.2.371>
- 809 Sanderson, B.M., Knutti, R. & Caldwell, P. (2015) A Representative Democracy to Reduce
810 Interdependency in a Multimodel Ensemble. *Journal of Climate*, 28, 5171–5194.
811 <https://doi.org/10.1175/jcli-d-14-00362.1>
- 812 Scherrer, D., & Körner, C. (2011). Topographically controlled thermal-habitat
813 differentiation buffers alpine plant diversity against climate warming. *Journal of*
814 *biogeography*, 38, 406–416. <https://doi.org/10.1111/j.1365-2699.2010.02407.x>
- 815 Skarpaas, O., Stabbe, O. E., Rønning, I., & Sverdrup, T. O. (2004). How far can a
816 hawk's beard fly? Measuring and modelling the dispersal of *Crepis praemorsa*. *Journal of*
817 *Ecology*, 92(5), 747–757. <https://doi.org/10.1111/j.0022-0477.2004.00915.x>
- 818 Sklenář, P., & Jørgensen, P. M. (1999). Distribution patterns of páramo plants in Ecuador.
819 *Journal of Biogeography*, 26, 681–691. <https://doi.org/10.1046/j.1365-2699.1999.00324.x>

- 820 Sklenář, P., & Ramsay, P. M. (2001). Diversity of zonal páramo plant communities in
821 Ecuador. *Diversity and Distributions*, 7, 113–124. <https://doi.org/10.1046/j.1472-4642.2001.00101.x>
- 823 Sklenář, P., Hedberg, I., & Cleef, A. M. (2014). Island biogeography of tropical alpine floras.
824 *Journal of Biogeography*, 41, 287–297. <https://doi.org/10.1111/jbi.12212>
- 825 Singer, A., Johst, K., Banitz, T., Fowler, M. S., Groeneveld, J., Gutiérrez, A. G., ... & Meyer,
826 K. M. (2016). Community dynamics under environmental change: How can next generation
827 mechanistic models improve projections of species distributions?. *Ecological Modelling*,
828 326, 63–74. <https://doi.org/10.1016/j.ecolmodel.2015.11.007>
- 829 Smith, S. J., Edmonds, J., Hartin, C. A., Mundra, A., & Calvin, K. (2015). Near-term
830 acceleration in the rate of temperature change. *Nature Climate Change*, 5, 333.
831 <https://doi.org/10.1038/nclimate2552>
- 832 Steinbauer, M. J., Grytnes, J. A., Jurasinski, G., Kulonen, A., Lenoir, J., Pauli, H., ... & Wipf,
833 S. (2018). Accelerated increase in plant species richness on mountain summits is linked to
834 warming. *Nature*, 556, 231. <https://doi.org/10.1038/s41586-018-0005-6>
- 835 Tamme, R., Götzenberger, L., Zobel, M., Bullock, J. M., Hooftman, D. A., Kaasik, A., &
836 Pärtel, M. (2014). Predicting species' maximum dispersal distances from simple plant traits.
837 *Ecology*, 95, 505–513. <https://doi.org/10.1890/13-1000.1>
- 838 Team, C. W., Pachauri, R. K., & Meyer, L. A. (2014). IPCC, 2014: climate change 2014:
839 synthesis report. Contribution of Working Groups I, II and III to the Fifth Assessment Report
840 of the intergovernmental panel on Climate Change. IPCC, Geneva, Switzerland, 151.
- 841 Thomson, F. J., Moles, A. T., Auld, T. D., & Kingsford, R. T. (2011). Seed dispersal distance
842 is more strongly correlated with plant height than with seed mass. *Journal of Ecology*, 99(6),
843 1299–1307. <https://doi.org/10.1111/j.1365-2745.2011.01867.x>
- 844 Thomson, F. J., Letten, A. D., Tamme, R., Edwards, W., & Moles, A. T. (2017). Can
845 dispersal investment explain why tall plant species achieve longer dispersal distances than
846 short plant species?. *New Phytologist*, 217(1), 407–415. <https://doi.org/10.1111/nph.14735>
- 847 Thuiller, W., Albert, C., Araújo, M. B., Berry, P. M., Cabeza, M., Guisan, A., ... & Sykes,
848 M. T. (2008). Predicting global change impacts on plant species' distributions: future
849 challenges. *Perspectives in plant ecology, evolution and systematics*, 9(3-4), 137–152.
850 <https://doi.org/10.1016/j.ppees.2007.09.004>
- 851 Thuiller, W., Georges, D., Engler, R., Breiner, F., Georges, M. D., & Thuiller, C. W. (2016).
852 Package 'biomod2'. Species distribution modeling within an ensemble forecasting
853 framework <https://CRAN.R-project.org/package=biomod2>.
- 854 Thuiller, W., Guéguen, M., Renaud, J., Karger, D. N., & Zimmermann, N. E. (2019).
855 Uncertainty in ensembles of global biodiversity scenarios. *Nature communications*, 10,
856 1446. <https://doi.org/10.1038/s41467-019-09519-w>
- 857 Tovar, C., Arnillas, C. A., Cuesta, F., & Buytaert, W. (2013). Diverging responses of tropical
858 Andean biomes under future climate conditions. *PloS one*, 8, e63634.
859 <https://doi.org/10.1371/journal.pone.0063634>

- 860 Travis, J. M., Delgado, M., Bocedi, G., Baguette, M., Bartoń, K., Bonte, D., ... &
861 Saastamoinen, M. (2013). Dispersal and species' responses to climate change. *Oikos*,
862 122(11), 1532–1540. <https://doi.org/10.1111/j.1600-0706.2013.00399.x>
- 863 Urrutia, R., & Vuille, M. (2009). Climate change projections for the tropical Andes using a
864 regional climate model: Temperature and precipitation simulations for the end of the 21st
865 century. *Journal of Geophysical Research: Atmospheres*, 114(D2).
866 <https://doi.org/10.1029/2008JD011021>
- 867 Visser, M. E., & Both, C. (2005). Shifts in phenology due to global climate change: the need
868 for a yardstick. *Proceedings of the Royal Society B: Biological Sciences*, 272, 2561–2569.
869 <https://doi.org/10.1098/rspb.2005.3356>
- 870 Vittoz, P., & Engler, R. (2007). Seed dispersal distances: A typology based on dispersal
871 modes and plant traits. *Botanica Helvetica*, 117, 109–124. [https://doi.org/10.1007/s00035-](https://doi.org/10.1007/s00035-007-0797-8)
872 [007-0797-8](https://doi.org/10.1007/s00035-007-0797-8)
- 873 Vittoz, P., Dussex, N., Wassef, J., & Guisan, A. (2009) Diaspore traits discriminate good
874 from weak colonisers on high-elevation summits. *Basic and Applied Ecology*, 10, 508–515.
875 <https://doi.org/10.1016/j.baae.2009.02.001>
- 876 Wisz, M. S., Pottier, J., Kissling, W. D., Pellissier, L., Lenoir, J., Damgaard, C. F., ... &
877 Svenning, J. C. (2013). The role of biotic interactions in shaping distributions and realised
878 assemblages of species: implications for species distribution modelling. *Biological reviews*,
879 88, 15–30. <https://doi.org/10.1111/j.1469-185X.2012.00235.x>

880 **Tables**

881 **Table 1:** Evaluation metrics and their standard deviation (in parenthesis) showing the overall
 882 performance of the GLM and RF models for 435 plant species as well as their comparison
 883 between algorithm according to a paired t-student test.

	TSS	Sensitivity	Specificity	Percentage of models kept (over 50 runs)
GLM	0.574 (0.17)	79.483 (11.85)	81.520 (13.03)	23.171 (15.79)
RF	0.652 (0.16)	82.171 (10.40)	80.477 (10.40)	28.891 (15.73)
Significant differences between algorithms	SI (t = -14.487, df = 432, p- value < 2.2e-16)	SI (t = -4.1044, df = 432, p-value = 4.846e-05)	NO (t = 1.6303, df = 432, p-value = 0.1038)	SI (t = -11.812, df = 432, p-value < 2.2e-16)

884

885 **Table 2:** Composition changes (in %) in terms of proportions of mid-páramo and super-
 886 páramo species at the sky island level between 2000 and 2100. The final super-páramo
 887 balance shows net gain (in green) or loss (in red) of super-páramo species, expressed as a
 888 percentage.

	2000		2100			Final super-páramo balance
	Mid-páramo species	Super-paramo species	Mid-páramo species	Super-páramo species	Standard deviation	
Altar	66.91	33.09	74.54	25.46	4.15	-7.63
Antisana	67.30	32.70	75.30	27.70	6.67	-8.01
Cajas	81.82	18.18	84.21	15.79	6.10	-2.39
Cayambe	69.33	30.67	68.56	31.44	4.16	+0.78
Chimborazo	64.47	35.53	71.15	28.85	2.40	-6.68
Cotopaxi	67.11	32.89	71.16	28.84	1.72	-4.04
Ilinizas	59.78	40.22	69.55	30.45	7.35	-9.76
Pichincha	69.90	30.10	73.77	26.23	13.44	-3.87
Sangay	75.51	24.49	75.99	24.01	5.33	-0.48
Tungurahua	65.75	34.25	71.92	28.08	6.99	-6.17

889

890

891 **Figure captions**

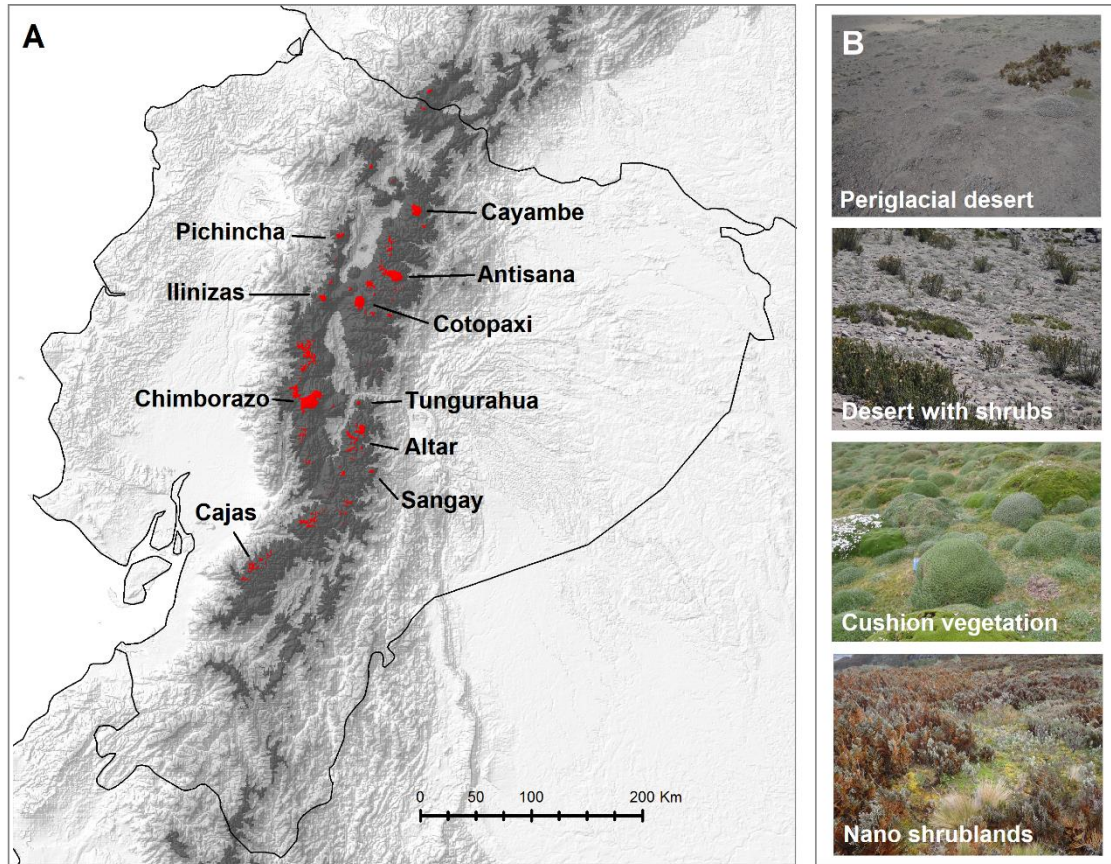
892 Figure 1: Current potential distribution of the páramo in Ecuador (A): in dark gray, mid-
893 páramo (3000-4200 m) and in red, super-páramo (> 4200 m); and characteristic super-
894 páramo vegetation (B), from bottom to top, increasing with elevation.

895 Figure 2: Examples of distribution responses of páramo species to climate change by 2100,
896 according to the CIMC5-RCP45-CESM1-BGC scenario: A) a mid-páramo species
897 colonizing higher elevations (*Vicia andicola*) and B) a super-páramo species reducing its
898 distribution (*Astragalus geminiflorus*).

899 Figure 3: Net richness changes at the pixel level (1 km²) between 2000 and 2100 in the 10
900 páramo sky islands above 4200 m (named in bold). Between parenthesis, balance of gained
901 and lost species between the present and 2100 (in percentage of the original richness at the
902 sky island level).

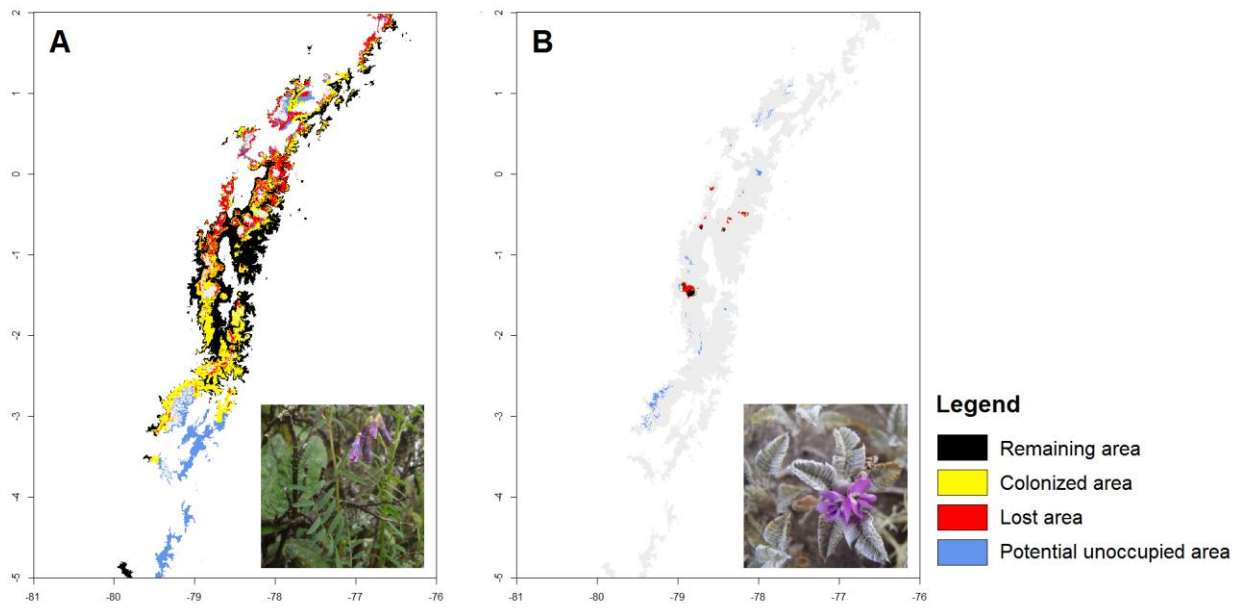
903 **Figures**

904 Figure 1



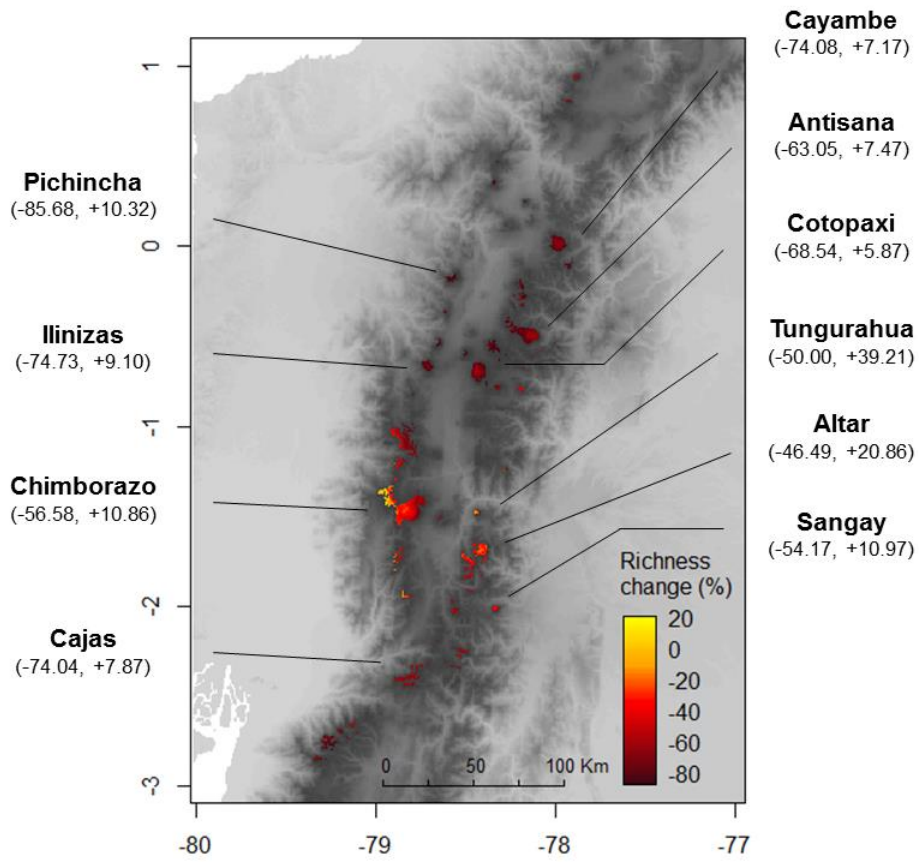
905

906 Figure 2



907

908 Figure 3



909

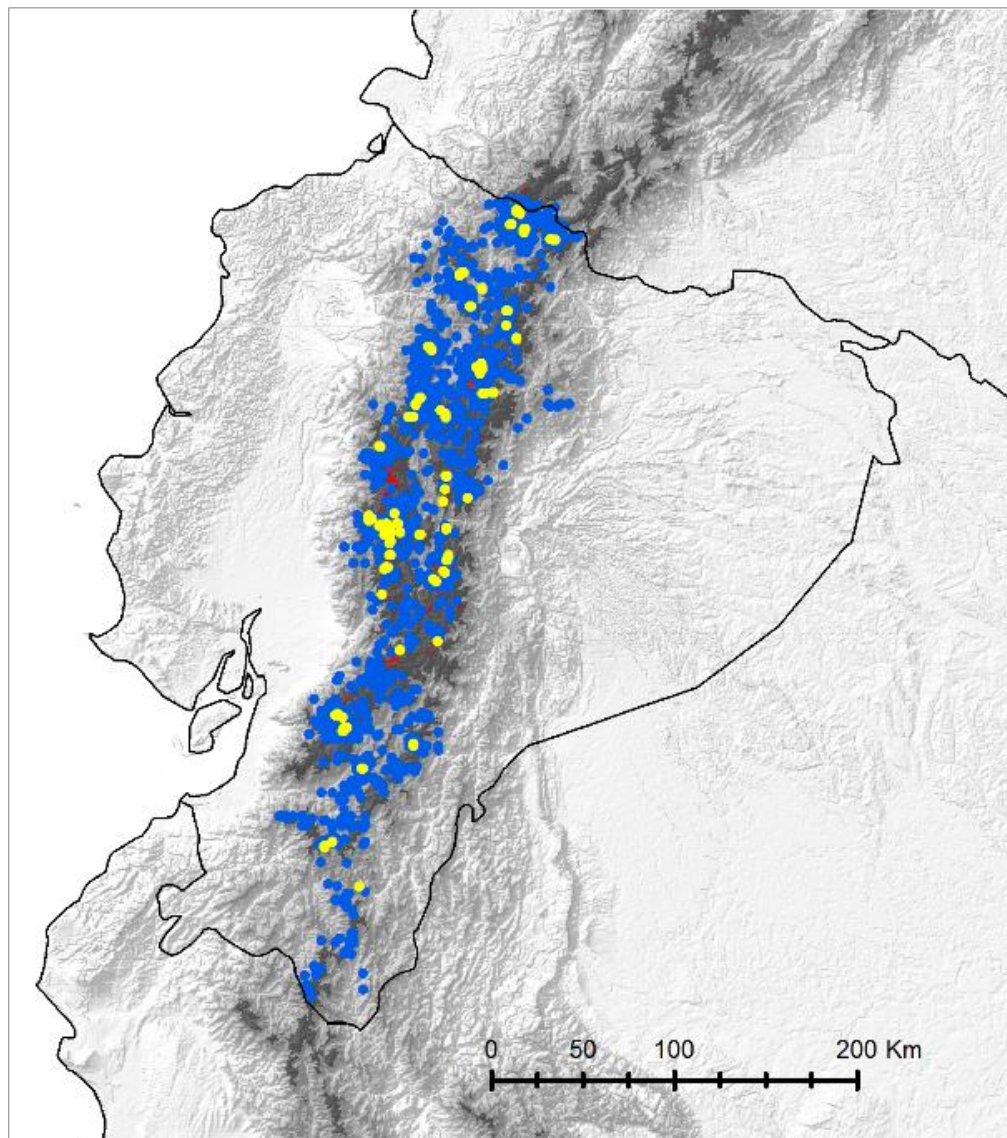
910 **Supplementary materials**

911 Table S1: vegetation and occurrence data used in this study (Peyre, 2020)

912 Table S2: List of species included in the analysis, including their representation in the final
913 dataset, mid-páramo versus super-páramo status and calculated maximum dispersal distance
914 (in m/yr).

915 Tabla S3: Species composition of the Ecuadorian sky islands for 2000 and 2100 according
916 to the modelling analyses and under the different climate change scenarios.

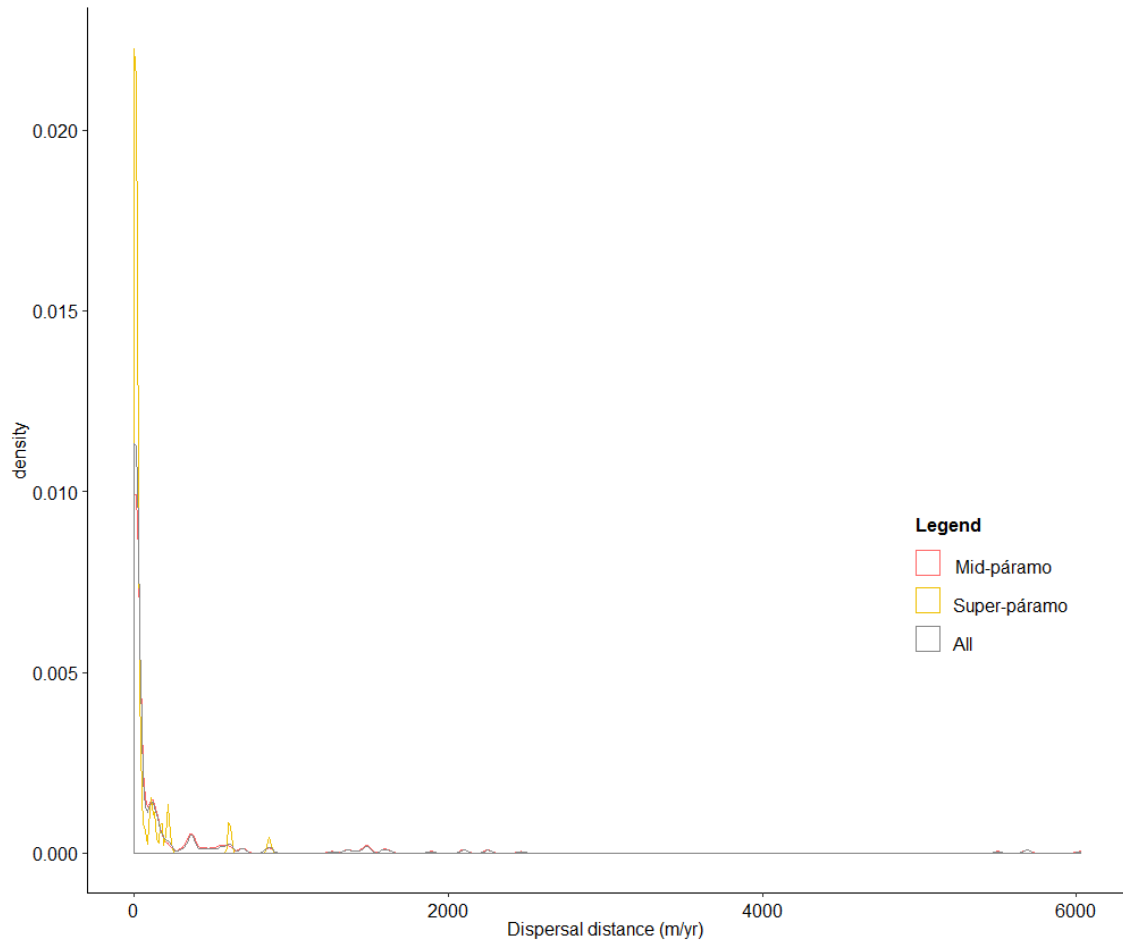
917 Figure S1: Distribution of the VegParamo plots (yellow) and additional data points (in blue)
918 across the study area.



919

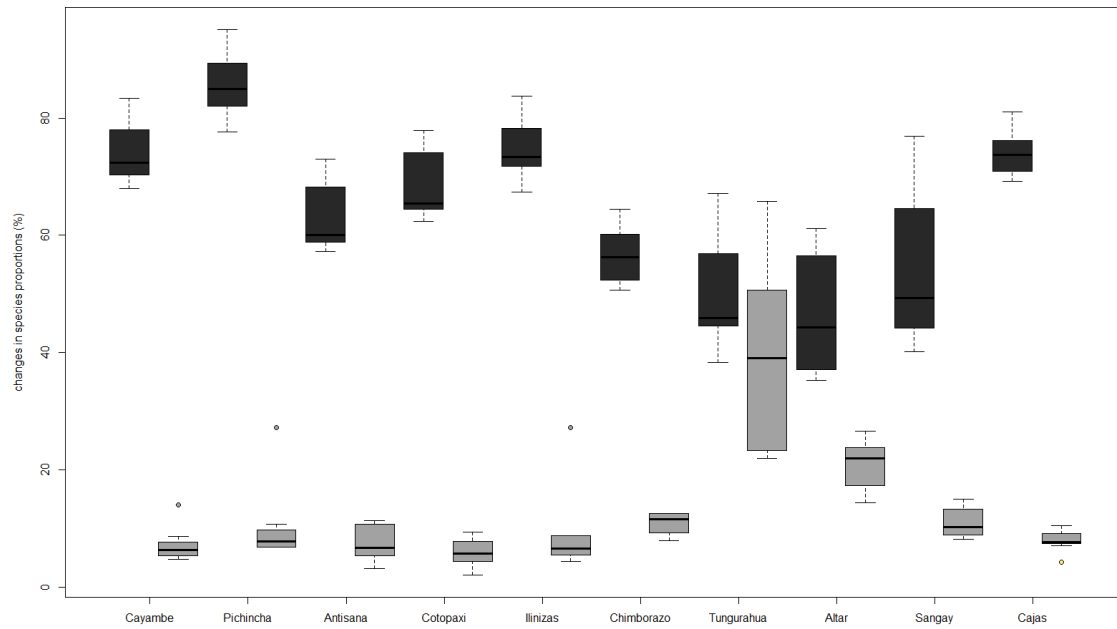
920

921 Figure S2: Density plot of the dispersal capacity, as maximum dispersal distance, of the
922 páramo species (m/yr), differentiating the mid-páramo and super-páramo species.
923



924

925 Figure S3: Balance of gained and lost species on the Ecuadorian sky islands between the
926 present and 2100 (in percentage of the original richness at the sky island level). Dark colours
927 represent lost species and light colours gained species.



928